Supporting Information

Smart Manganese Dioxide-Based Lanthanide Nanoprobes for Triple-Negative Breast Cancer Precise Gene Synergistic Chemodynamic Therapy

Liyan Ming[1,2], Liang Song[1,2,3], Jixuan Xu[1,2], Ruoping Wang[1,2], Junpeng Shi[1,2,3], Min Chen[4] and Yun Zhang[1,2,3,5]**

[1]CAS Key Laboratory of Design and Assembly of Functional Nanostructures, and Fujian Provincial Key Laboratory of Nanomaterials, Fujian Institute of Research on the Structure of Matter, Chinese Academy of Sciences, Fuzhou 350002, China

[2]Xiamen Institute of Rare Earth Materials, Haixi Institute, Chinese Academy of Sciences, Xiamen Key Laboratory of Rare Earth Photoelectric Functional Materials, Xiamen 361021, China

[3]Ganjiang Innovation Academy, Chinese Academy of Sciences, Jiangxi 341000, China

[4]Clinical Central Research Core, Key Laboratory for Endocrine-Related Cancer Precision Medicine of Xiamen, Xiangan Hospital of Xiamen University, Cancer Research Center, School of Medicine, Xiamen University, Xiamen 361102, China

[5]University of Chinese Academy of Sciences, Beijing 100049, China

*Corresponding Author

Liang Song, E-mail: songliang@fjirsm.ac.cn and Yun Zhang, E-mail: zhangy@fjirsm.ac.cn.

Tel: +86 0592-3576133

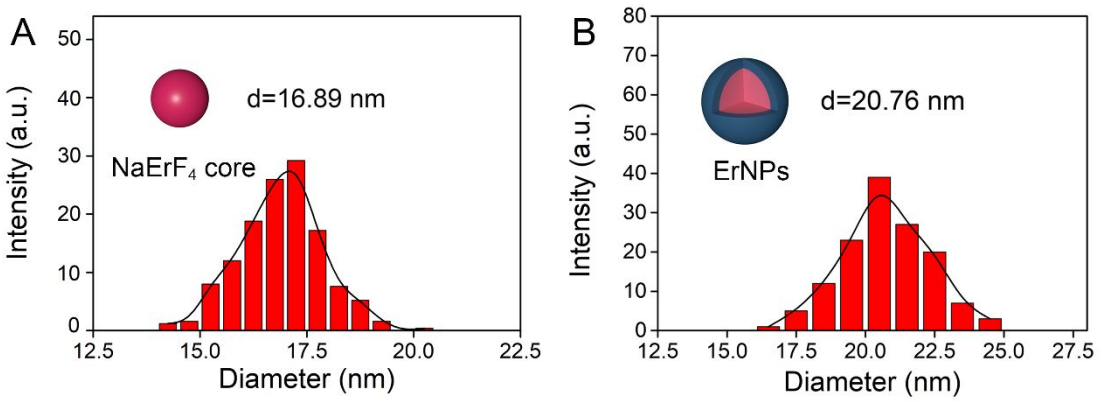

Figure S1. The size distribution of $NaErF_4$ core nanoparticles (A, d=16.89 nm) and ErNPs nanoprobes (B, d=20.76 nm).

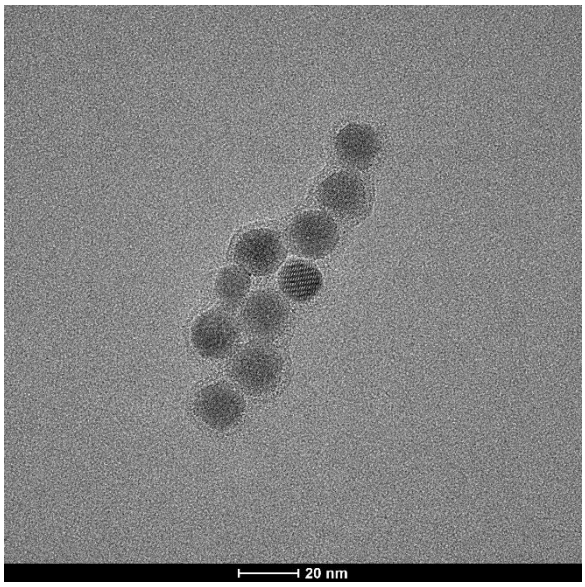

Figure S2. The TEM images of $NaErF_4$@$NaYF_4$@C nanoparticles.

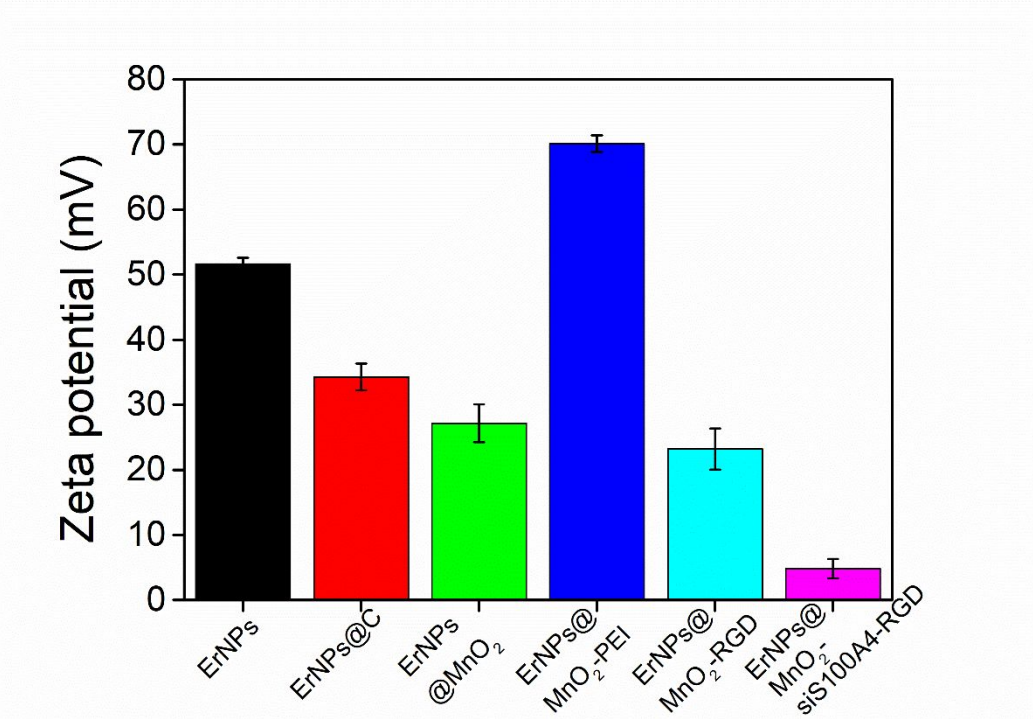

Figure S3. The zeta potential of ErNPs, ErNPs@C, ErNPs@MnO_2, ErNPs@MnO_2-PEI, ErNPs@MnO_2-RGD and ErNPs@MnO_2-siS100A4-RGD (n=3).

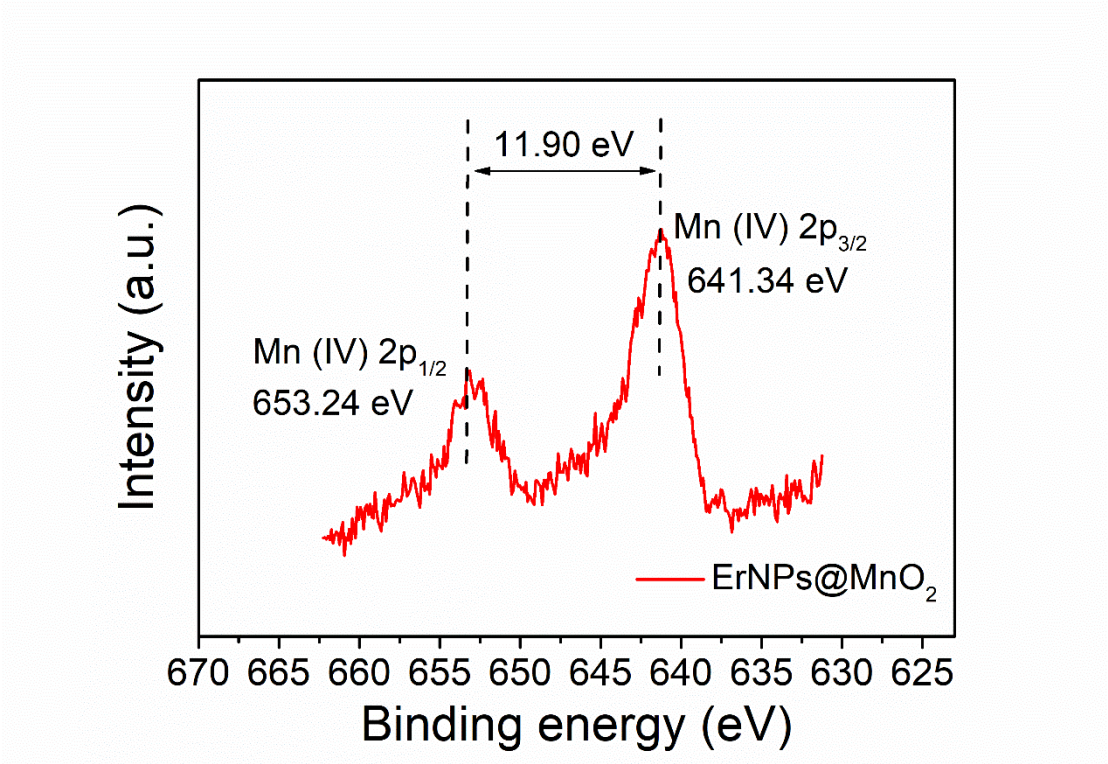

Figure S4. High resolution Mn 2p XPS spectrum of ErNPs@MnO_2.

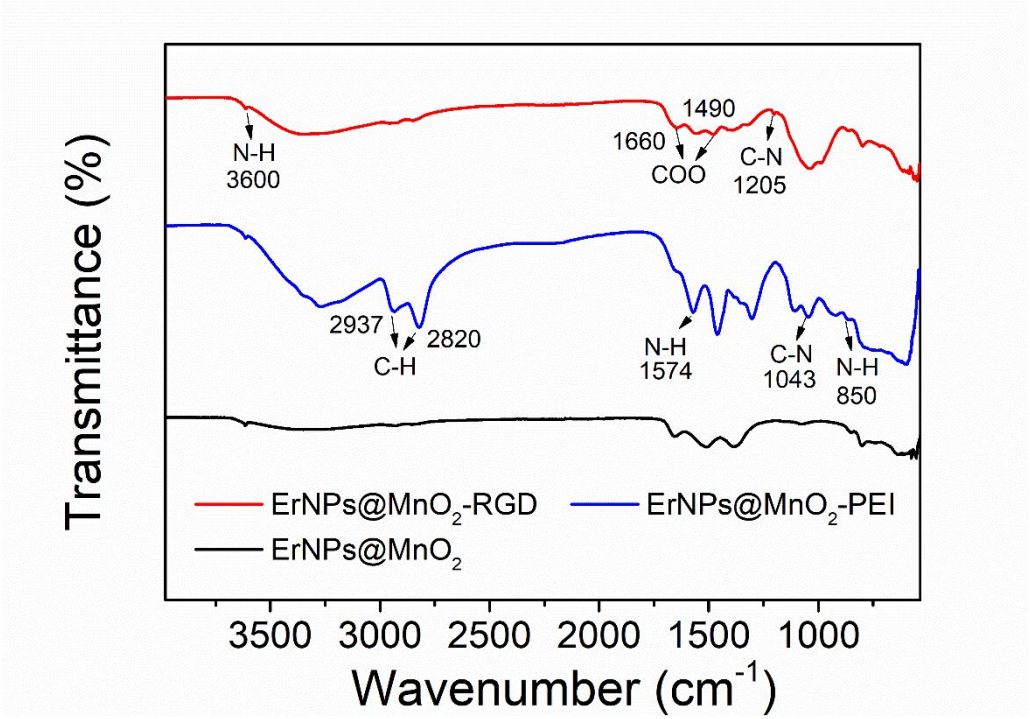

Figure S5. FT-IR spectra of ErNPs@MnO_2, ErNPs@MnO_2-PEI and ErNPs@MnO_2-RGD.

Figure S6. The released efficiency of siRNA form ErNPs@MnO_2-RGD nanoparticles treated with 10% SDS.

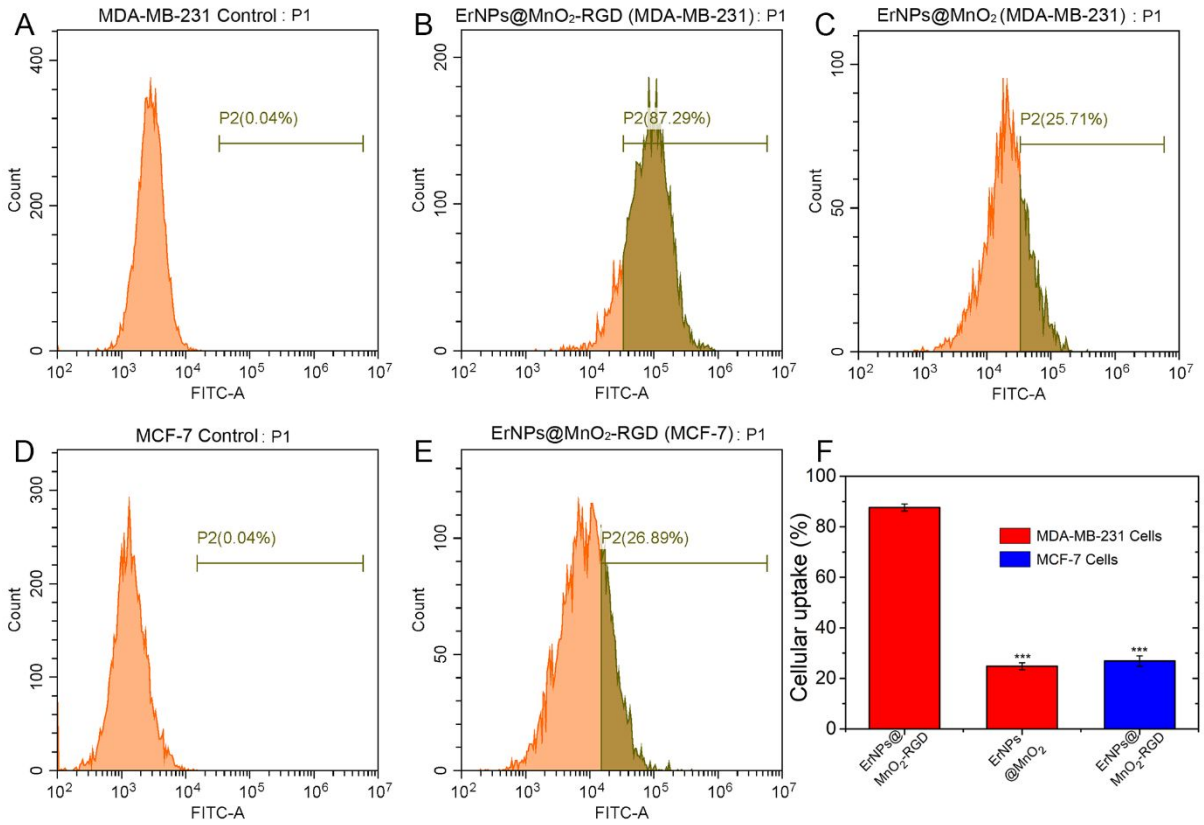

Figure S7. Analysis of material uptake rates by flow cytometry. The cellular uptake of MDA-MB-231 cells after treated with no treatment (A), ErNPs@MnO_2-RGD (B) and ErNPs@MnO_2 (C), and MCF-7 cells after treated with no treatment (D), ErNPs@MnO_2-RGD (E) respectively for 2 h. (F) The corresponding quantitative analysis (n=3, compared with MDA-MB-231 cells treated with ErNPs@MnO_2-RGD group, ***P<0.001).

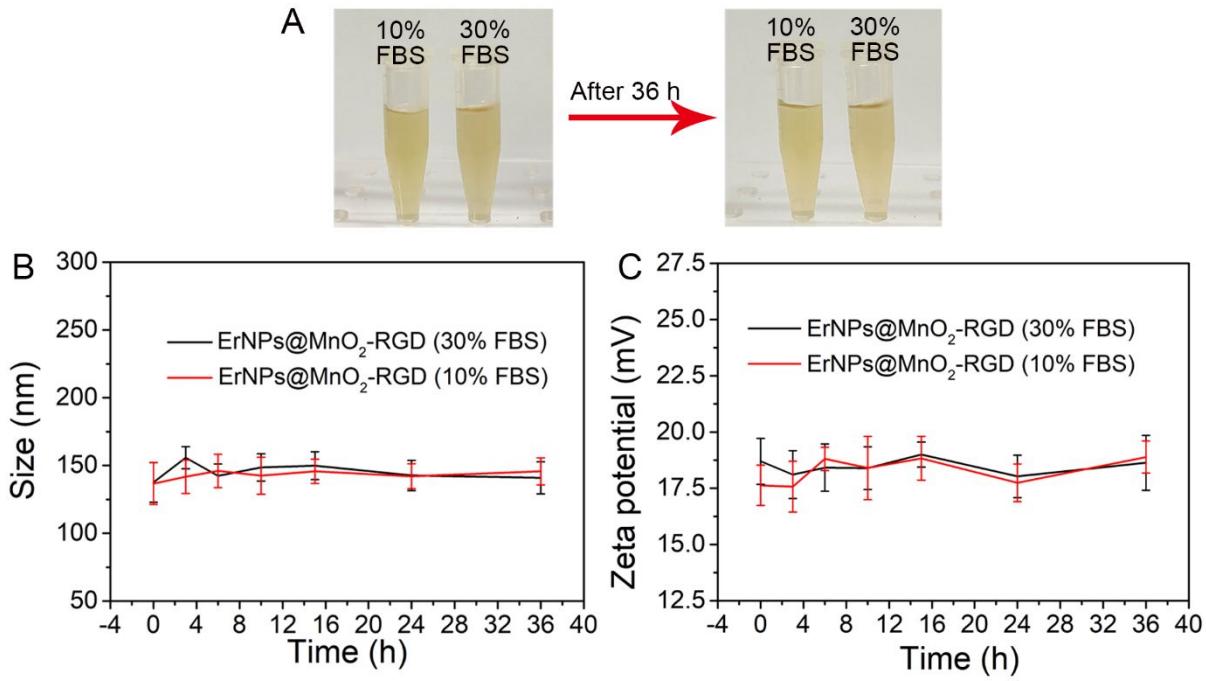

Figure S8. The stability of ErNPs@MnO_2-RGD in the serum environment. (A) Digital photo of ErNPs@MnO_2-RGD in PBS containing 10% or 30% FBS. (B) Size and (C) Zeta potential changes of ErNPs@MnO_2-RGD during 36 h in PBS containing 10% and 30% FBS, respectively (n=3).

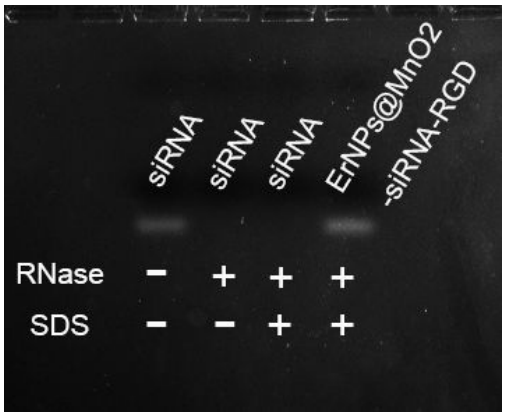

Figure S9. The stability of siRNA loaded on ErNPs@MnO_2-RGD nanoparticles. siS100A4 and ErNPs@MnO_2-siS100A4-RGD were treated with or without RNase at 37 °C for 1 h, analyzed by agarose gel electrophoresis.

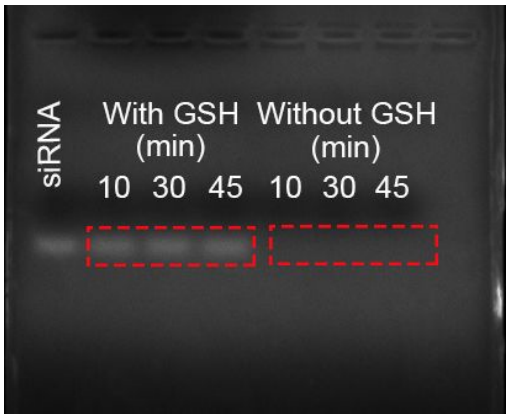

Figure S10. GSH-responsive siRNA release efficiency. ErNPs@MnO_2-siS100A4-RGD were treated with $NaHCO_3$/5% CO_2 buffer solution and H_2O_2 with or without GSH for 10, 30, 45 min, and analyzed by agarose gel electrophoresis.

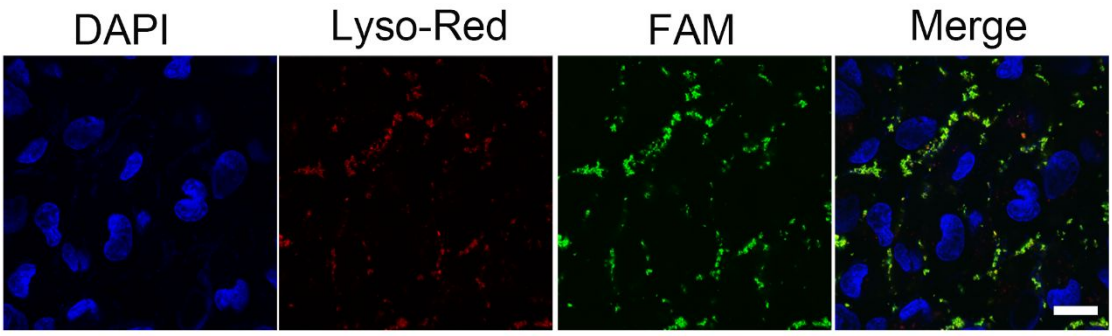

Figure S11. Endosome escape of ErNPs@MnO_2-siRNA-RGD in MDA-MB-231 cells. CLSM images of MDA-MB-231 cells incubated with FAM-siRNA loaded ErNPs@MnO_2 -RGD at 37 °C for 2 h (Scale bar: 20 μm).

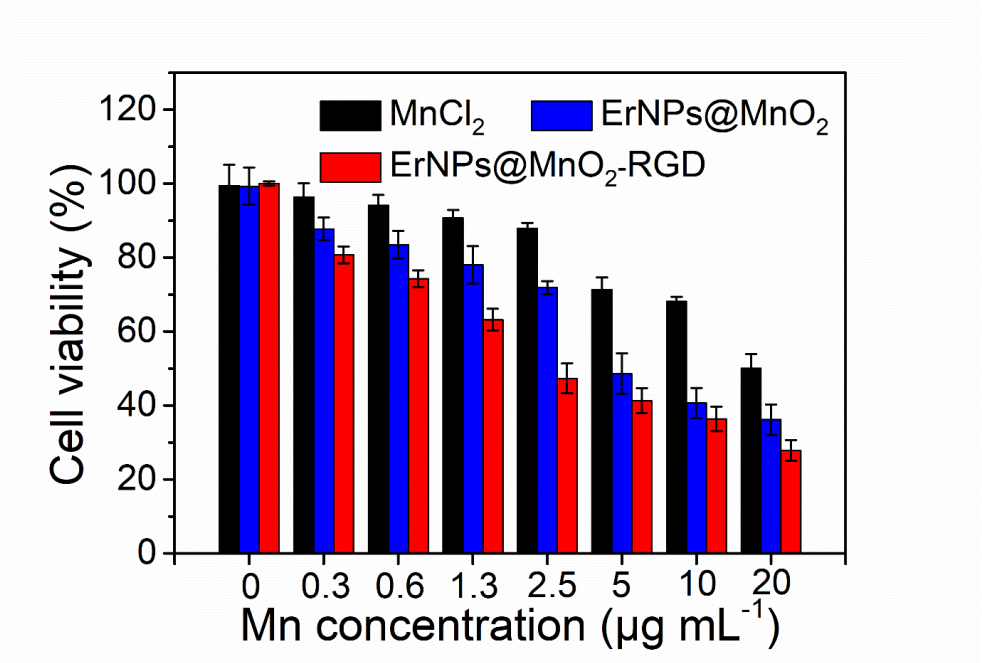

Figure S12. CDT effect of different concentrations of Mn^{2+}, ErNPs@MnO_2 and ErNPs@MnO_2-RGD (0, 0.3, 0.6, 1.3, 2.5, 5, 10, 20 μg mL^{-1} of Mn) on MDA-MB-231 cells (n=4).

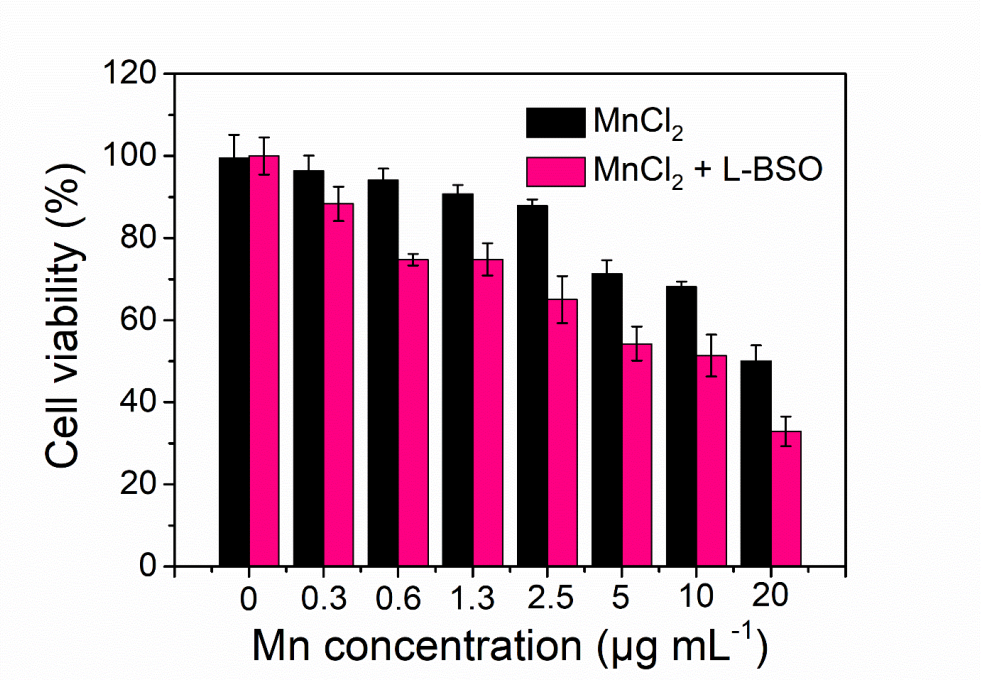

Figure S13. *In vitro* chemodynamic toxicity of Mn^{2+} with or without L-BSO after 24 h treatment (n=4).

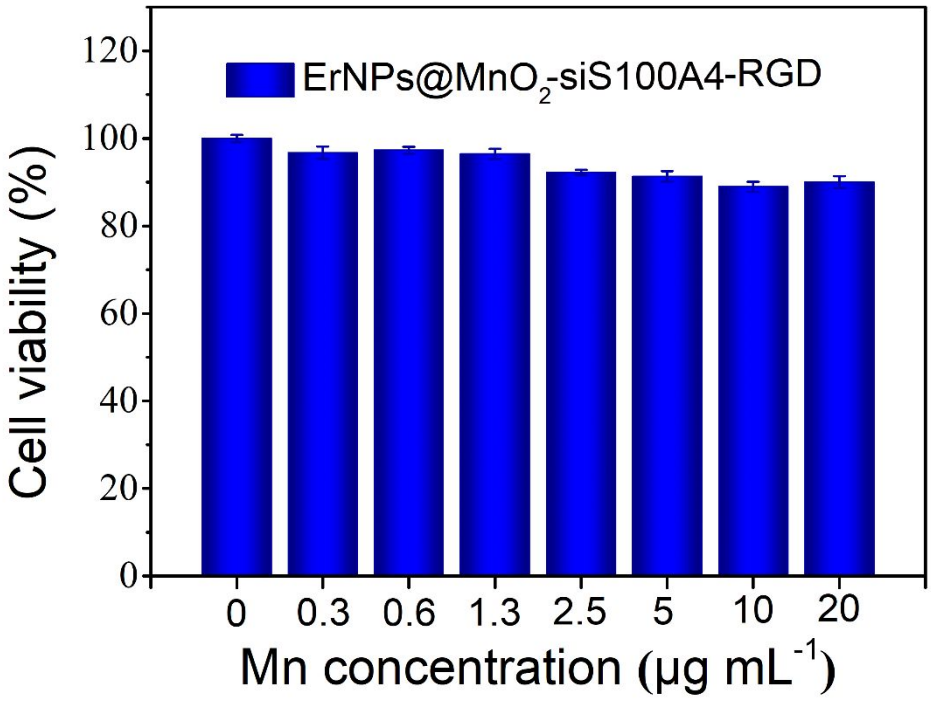

Figure S14. MCF-10A (common breast cells) cell viability treated with ErNPs@MnO_2-siS100A4-RGD for 24 h (n=4).

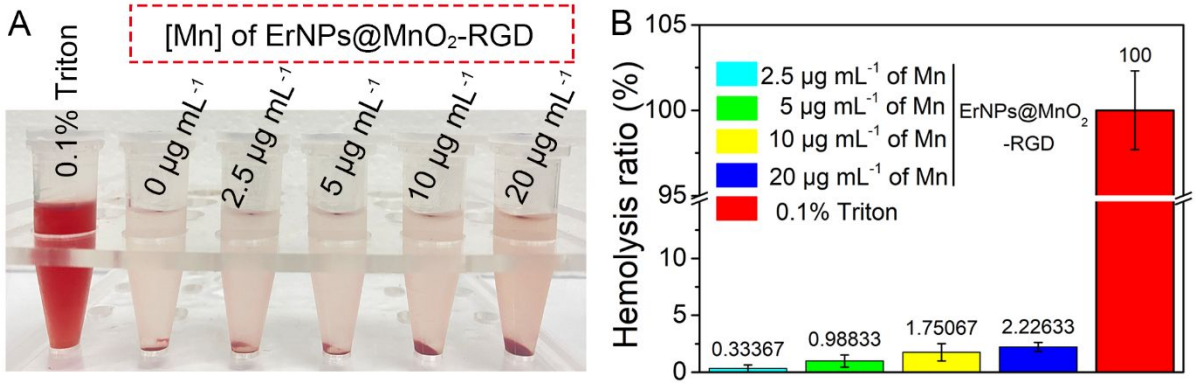

Figure S15. Hemolysis test. (A) Images of hemolysis test and (B) the corresponding hemolysis rate of ErNPs@MnO_2-RGD at different concentrations of Mn.

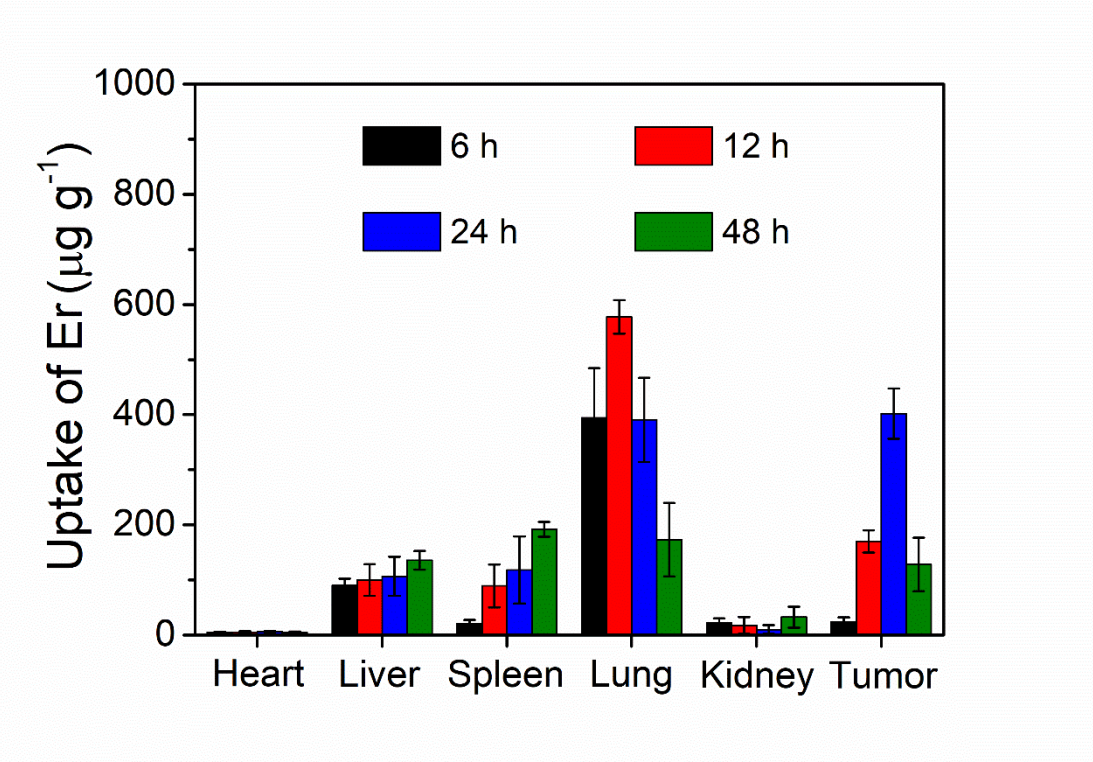

Figure S16. *In vivo* distribution of ErNPs@MnO_2-RGD in MDA-MB-231 tumor-bearing nude mice with different times after injection (n=3).

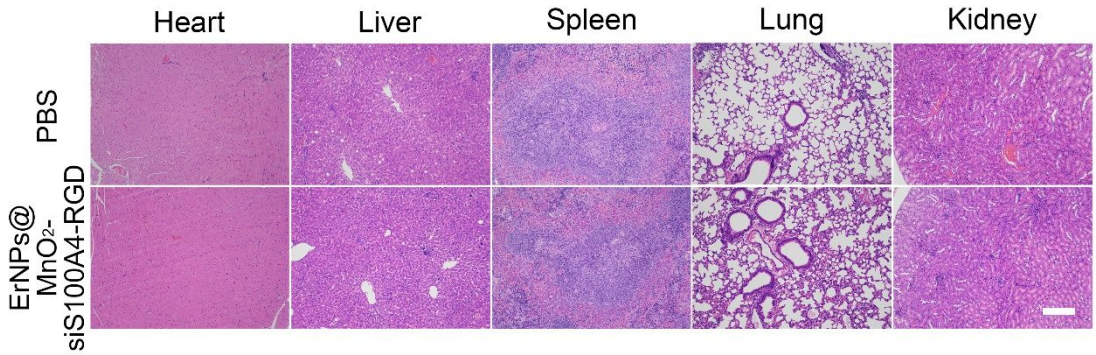

Figure S17. Microscopy images of H&E stained slices of major organs extracted 25 days after vein injection of PBS and ErNPs@MnO_2-siS100A4-RGD, respectively (scale bar: 100 μm).

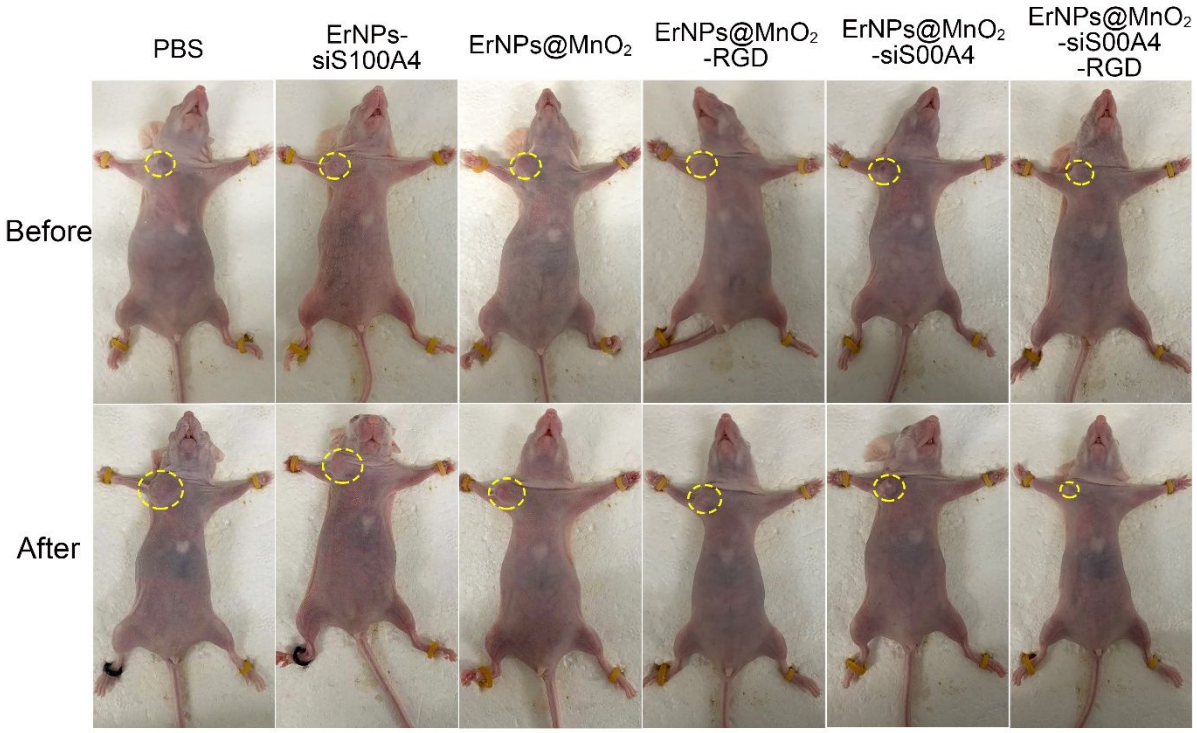

Figure S18. *In vivo* tumor therapeutic efficiency with the changes of tumor images after treated with no treatment, ErNPs-siS100A4, ErNPs@MnO_2, ErNPs@MnO_2 -RGD, ErNPs@MnO_2-siS100A4, ErNPs@MnO_2-siS100A4-RGD.

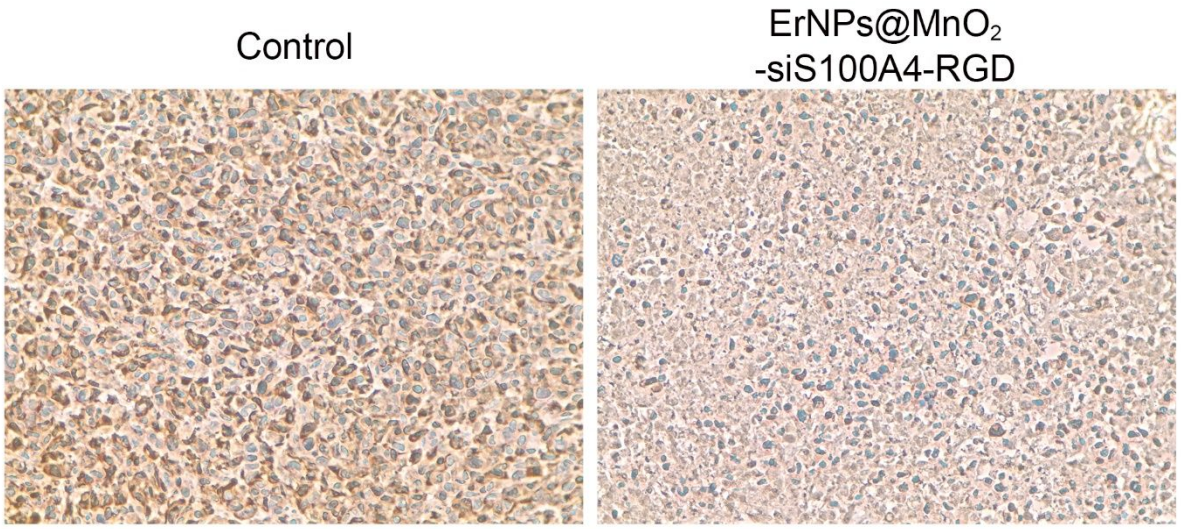

Figure S19. Microscopy images of immunohistochemical analysis of S100A4 expression in

tumor sites after treated with PBS and ErNPs@MnO_2-siS100A4-RGD, respectively (400 x microscope photos), dark brown represents histochemical staining, blue represents the cell nucleus.

Table S1. The polydispersity index of ErNPs@MnO_2-RGD in the serum environment

Time (h)	ErNPs@MnO_2-RGD in 10% FBS	ErNPs@MnO_2-RGD in 30% FBS
0	0.172	0.178
3	0.141	0.183
10	0.198	0.205
15	0.165	0.197
24	0.176	0.163
36	0.197	0.212